

Neutrino masses and particle physics beyond the standard model

Heinrich Päs

Institut für Theoretische Physik und Astrophysik
Universität Würzburg
Am Hubland, 97074 Würzburg, Germany
paes@physik.uni-wuerzburg.de

Received 01.07.2002, accepted dd.mm.yyyy by ue

Abstract. The evidence for non-vanishing neutrino masses from solar and atmospheric neutrinos provides the first solid hint towards physics beyond the standard model. A full reconstruction of the neutrino spectrum may well provide a key to the theoretical structures underlying the standard model such as supersymmetry, grand unification or extra space dimensions. In this article we discuss the impact of absolute neutrinos masses on physics beyond the standard model. We review the information obtained from neutrino oscillation data and discuss the prospects of the crucial determination of the absolute neutrino mass scale, as well as the intriguing connection with the Z-burst model for extreme-energy cosmic rays.

Keywords: Neutrino mass, beyond the standard model, unification

PACS: 12.60.-i, 14.60.Pq

1 Introduction

The ultimate goal of particle physics is the quest for unification in a final theory underlying the standard model (SM), which describes the present knowledge about physics at low energies. So far the only experimental hint for new physics beyond the SM has been provided by solar and atmospheric neutrino experiments which have established solid evidence for non-vanishing neutrino masses. This article aims to be a pedagogical introduction to the specific role of the neutrino among the elementary fermions and what can be learned from future neutrino experiments about the theoretical structures underlying the SM (for more detailed excellent reviews on the topic see also [1, 2]). A crucial ingredient for the reconstruction of theories beyond the SM will be a determination of the absolute mass scale for neutrinos, which is still unknown [3]. In fact, it is an experimental challenge to determine an absolute neutrino mass below 1 eV. Three approaches have the potential to accomplish the task, namely larger versions of the tritium end-point distortion measurements, limits from the evaluation of the large scale structure of the universe, and next-generation neutrinoless double beta decay ($0\nu\beta\beta$) experiments. In addition, there is a fourth possibility: the extreme-energy cosmic-ray experiments in the context of the recently emphasized Z-burst model.

This article is organized as follows: In section 2 the basic ideas of supersymmetry, grand unification, and large extra dimensions are mentioned. Section 3 deals with

the specific role of the neutrino among the elementary fermions of the SM, as well as with the two most popular mechanisms for neutrino mass generation. Also, the link of absolute neutrino masses to the theory underlying the SM is discussed. Section 4 reviews the experimental evidence for non-vanishing neutrino masses from neutrino oscillations and the knowledge about the neutrino mass matrix. Section 5 deals with direct determinations of the absolute neutrino mass via tritium beta decay and cosmology. In section 6 we discuss the $0\nu\beta\beta$ which may test very small values of neutrino masses, when information is input obtained from oscillation studies. Section 7 finally deals with the connection of the sub-eV neutrino mass scale and the ZeV energy scale of extreme energy cosmic rays in the Z-burst model.

2 The holy grail of particle physics

The final goal of particle physics is the unification of particles and forces in a fundamental framework. The low energy particle content of the SM consists of three families (flavors) of quarks

$$\begin{pmatrix} u_L \\ d_L \end{pmatrix}, \begin{pmatrix} c_L \\ s_L \end{pmatrix}, \begin{pmatrix} t_L \\ b_L \end{pmatrix}, u_R, d_R, c_R, s_R, t_R, b_R \quad (1)$$

and leptons

$$\begin{pmatrix} e_L \\ \nu_e \end{pmatrix}, \begin{pmatrix} \mu_L \\ \nu_\mu \end{pmatrix}, \begin{pmatrix} \tau_L \\ \nu_\tau \end{pmatrix}, e_R, \mu_R, \tau_R. \quad (2)$$

The left handed fermions transform as doublets under the electroweak SU(2) gauge group, the right handed counterparts are singlets, and no right-handed neutrinos are included in the SM. To preserve gauge invariance, fermion masses are understood as symmetry breaking effects due to couplings to the vacuum expectation value (vev) of the Higgs doublet - in analogy to the effective photon masses generated in superconductors.

The effective interactions at low energies are electromagnetism, weak and strong interactions which are mediated by gauge bosons. In the sense of unification, the running of the coupling strengths, due to vacuum polarization effects of these interactions, are traced to higher energies and unification is assumed at the grand unified theory (GUT) scale (see Fig. 1). In this picture, physics at low energies is described by the SM, around 1 TeV supersymmetry enters, and at some 10^{16} GeV unification is realized. Large extra space dimensions may complement this picture and can, in some respects, be considered as an alternative to low energy supersymmetry.

2.1 Supersymmetry

Supersymmetry (SUSY) is a hypothetical symmetry between bosons and fermions in the sense that each elementary fermion f acquires a superpartner, a scalar fermion (sfermion) \tilde{f} , and each gauge or Higgs boson gets a spin 1/2 gaugino or Higgsino partner. The inclusion of these new degrees of freedom at the SUSY breaking scale of about 1 TeV allows the gauge couplings to unify. Supersymmetry would also cancel

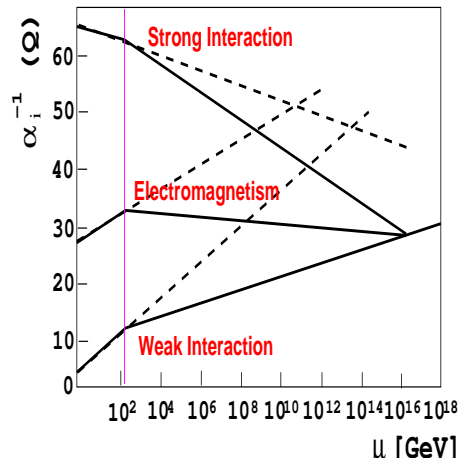


Fig. 1 Running coupling constants: With increasing energy the couplings of the electromagnetic, strong and weak interactions evolve, are supposed to change directions at the SUSY scale of about 1 TeV, and are finally assumed to unify at the unification scale.

divergencies of the SM and would offer a candidate for the spurious dark matter of the universe, provided the lightest supersymmetric particle is stable. Moreover, it would offer a natural and promising approach for developing a consistent quantum theory of gravity.

2.2 Grand Unification

At the unification scale, the three interactions are assumed to unify and the elementary fermions to be accommodated in large multiplets. In this way a higher level of symmetry is restored in the theory. Typical issues are lepton and baryon (quark) number violation due to transitions between leptons and quarks in the same multiplet and the prediction of right handed neutrinos.

2.3 Extra Space-Dimensions

Extra dimensions beyond the three space and one time dimensions of the low energy world are predicted in string theories which aim at a consistent quantum theory of gravity. Such extra dimensions can be large (up 0.1 mm size, for example) if the fermions of the SM are confined on a three dimensional brane and only gravitons and SM singlets can propagate in the extra-dimensional bulk. Such theories have interesting predictions for the energy scales of unification, the quantum gravity scale, and neutrino physics.

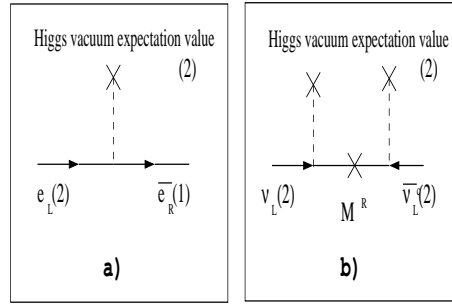


Fig. 2 Diagrams for Dirac masses via couplings to the Higgs vacuum expectation value (panel a) and effective Majorana neutrino masses via couplings to the Higgs vev and a heavy right-handed neutrino singlet (panel b).

3 Neutrino masses and physics beyond the standard model

The specific role of the neutrino among the elementary fermions of the SM is twofold: It is the only neutral particle, and its mass is much smaller than the masses of the charged fermions. Thus these properties may be related within a deeper theoretical framework underlying the SM – usually via Majorana mass-generating mechanisms. Such lepton number violating Majorana masses connect particle and antiparticle degrees of freedom and are thus obviously forbidden for charged particles. In the following, we comment on the most popular mechanisms to generate small neutrino masses, namely the see-saw mechanism, radiative neutrino mass generation and large extra dimensions.

3.1 The see-saw mechanism

The see-saw mechanism [4] is based on the observation that in order to generate Dirac neutrino masses

$$m^D \overline{\nu}_L \nu_R \quad (3)$$

analogous to the mass terms of the charged leptons (see Fig. 2a), the introduction of right-handed SU(2) singlet neutrinos is required. However, a lepton-number violating, Majorana mass term for right-handed neutrinos

$$\overline{\nu}_R M^R (\nu_R)^c \quad (4)$$

is not prohibited by any gauge symmetry of the SM. Thus by buying a Dirac neutrino mass term m^D , one inevitably invites mixing with a Majorana mass $M^R \gg m^D$ which may live, a priori, at the mass scale of the underlying unified theory. The diagonalization of the general mass matrix yields mass eigenvalues

$$m_\nu \simeq (m^D)^2 / M^R \ll m^D, \quad (5)$$

$$M \simeq M^R, \quad (6)$$

explaining the smallness of the light mass, which can be described by the effective operator corresponding to the diagram in Fig. 2b. The fundamental scale M^R is inaccessible for any kind of direct experimental testing. Nevertheless, it is obvious from eq. (5) that with information on the low-energy observables m_ν and m^D the “beyond the SM” mass scale of M^R can be reconstructed. While it turns out to be unrealistic to determine m^D in the SM, this option exists indeed in supersymmetry. In the supersymmetric version of the see-saw mechanism, lepton flavor violation (LFV) in the neutrino mass matrix (as required by neutrino oscillations) generates also LFV soft terms in the slepton mass matrix proportional to the Dirac neutrino Yukawa couplings [5],

$$\delta\tilde{m}_L^2 \propto Y_\nu Y_\nu^\dagger. \quad (7)$$

These LFV soft terms induce large branching ratios for SUSY mediated loop-decays such as $\mu \rightarrow e\gamma$,

$$\Gamma(\mu \rightarrow e\gamma) \propto \alpha^3 \frac{|\delta\tilde{m}_L^2|_{ij}^2}{m_S^8} \tan^2 \beta. \quad (8)$$

Here m_S denotes the slepton mass scale in the loop. Thus in the supersymmetric framework it is possible to probe the heavy mass scale M^R by determining the (light) neutrino mass scale m_ν and the (Dirac) Yukawa couplings. This fact is illustrated in Fig. 3, where computer simulation data of the branching ratio $\mu \rightarrow e\gamma$ are shown as a function of M^R for a specific SUSY (mSUGRA) scenario, both for a large (lower curve) and small (upper curve) neutrino mass scale [6].

3.2 Radiative neutrino masses

An alternative mechanism generates neutrino masses via loop graphs at the SUSY scale, in contrast to the tree level generation of charged lepton masses via the Higgs mechanism (see e.g. [7]). In supersymmetric theories lepton-number violating couplings, λ and λ' , may arise if the discrete R-parity symmetry is broken (\mathcal{R}_p). These couplings may induce neutrino masses via one loop self-energy graphs, see Fig. 4. The entries in the neutrino mass matrix, given by

$$m_{\nu_{ii'}} \simeq \frac{N_c \lambda'_{ijk} \lambda'_{i'kj}}{16\pi^2} m_{d_j} m_{d_k} \left[\frac{f(m_{d_j}^2/m_{d_k}^2)}{m_{\tilde{d}_k}} + \frac{f(m_{d_k}^2/m_{d_j}^2)}{m_{\tilde{d}_j}} \right], \quad (9)$$

are proportional to the products of \mathcal{R}_p -couplings and depend on the values of super-partner masses. A determination of the absolute neutrinos mass scale would allow one to constrain all entries in the mass matrix, using the smallness of atmospheric and solar Δm^2 's and unitarity of the neutrino mixing matrix U . In fact, recent bounds on absolute neutrino masses improve previous bounds on \mathcal{R}_p -couplings by up to 4 orders of magnitude [8]. Thus determining the neutrino mass probes physics at heavy mass scales beyond the SM also in the case of radiatively generated neutrino masses.

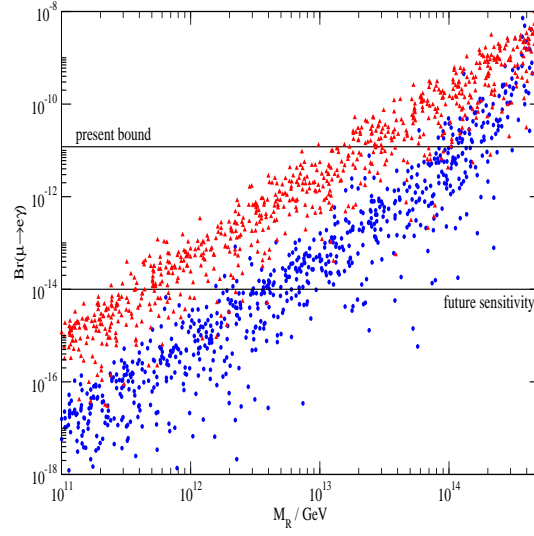


Fig. 3 Computer simulation of the branching ratio $\mu \rightarrow e\gamma$ as a function of the right-handed Majorana mass M^R . Shown are large (lower curve) and small (upper curve) neutrino mass scales, for a specific SUSY (mSUGRA) scenario. The scatter points correspond to estimated uncertainties in neutrino parameters after planned neutrino experiments have been performed (from [6]).

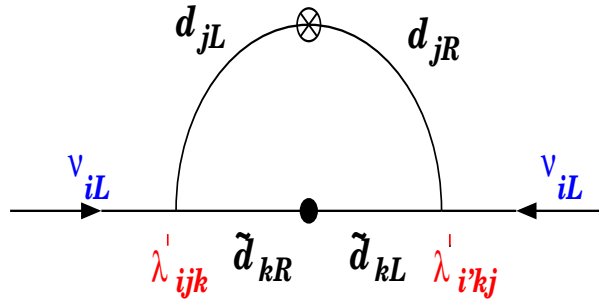


Fig. 4 Radiative generation of neutrino Majorana masses in R_p -violating SUSY.

3.3 Neutrino masses from large extra dimensions

In theories with large extra dimensions small neutrino masses may be generated by volume-suppressed couplings to right-handed neutrinos which can propagate in the bulk, by the breaking of lepton number on a distant brane, or by the curvature of the extra dimension [9]. Thus neutrino masses can provide information about the volume or the geometry of the large extra dimensions.

4 Experimental evidence: neutrino oscillations

Neutrino oscillations, i.e. oscillating flavor conversion, arise if the flavor states ν_α are superpositions of different non-degenerate mass eigenstates ν_i ,

$$|\nu_\alpha\rangle = \sum_i U_{\alpha i} |\nu_i\rangle. \quad (10)$$

In this case, a flavor eigenstate produced at one vertex propagates as a superposition of mass eigenstates (see Fig. 5),

$$|\nu_\alpha\rangle = \sum_i e^{-iE_i t} U_{\alpha i} |\nu_i\rangle, \quad (11)$$

with energies $E_i = \sqrt{p_i^2 + m_i^2}$. At a second vertex, there is the probability

$$\begin{aligned} P(\nu_\alpha \rightarrow \nu_\beta)(t) &= |\langle \nu_\beta | \nu_\alpha \rangle|^2 \\ &= \left| \sum_i e^{-iE_i t} U_{\alpha i} U_{\beta i}^* \right|^2 \end{aligned} \quad (12)$$

to observe a different flavor eigenstate $\nu_\beta \neq \nu_\alpha$. In a two neutrino framework, U can be parametrized as

$$U = \begin{pmatrix} \cos \theta & \sin \theta \\ -\sin \theta & \cos \theta \end{pmatrix}. \quad (13)$$

The oscillation probability becomes

$$P(\nu_\alpha \rightarrow \nu_\beta)(t) = \sin^2 2\theta \sin^2 \left[\frac{\Delta m^2}{4E} x \right], \quad (14)$$

with the propagation distance $x \simeq t$ and $E_i \simeq |\vec{p}| + \frac{m_i^2}{2|\vec{p}|} \simeq |\vec{p}|$. The two-neutrino approximation is a good approach to describe solar and atmospheric neutrino oscillations since the remaining mixing angle(s) are small.

4.1 Reactor neutrinos

An intense terrestrial source of low energy MeV $\bar{\nu}_e$ neutrinos is provided by nuclear reactors. Thus reactor neutrino experiments searching for $\bar{\nu}_e \rightarrow \bar{\nu}_\mu$ oscillations offer a possibility to test small Δm^2 's (compare eq. (14)). In the CHOOZ [10] and Palo Verde [11] experiments one didn't observe a disappearance signal. One has restricted the mixing matrix element to the small value of $U_{e3}^2 < 0.025$ or $\sin^2 2\theta_{13} < 0.1$, for $\Delta m_{13}^2 > 7 \times 10^{-4} \text{ eV}^2$. This bound is also important for the interpretation of the atmospheric neutrino anomaly.

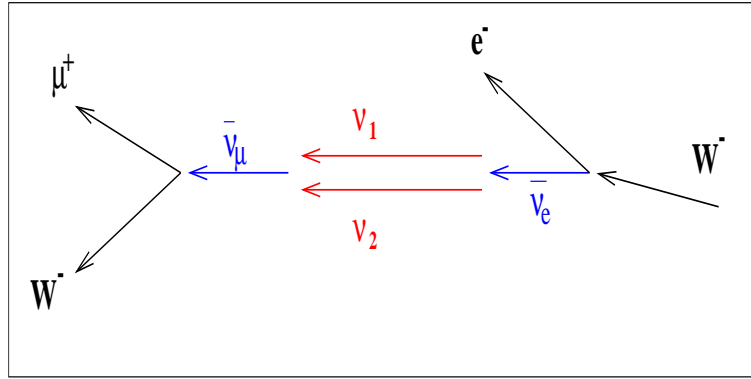


Fig. 5 Schematic diagram for neutrino oscillations.

4.2 Atmospheric neutrinos

Atmospheric neutrinos are produced in the decays of the π and K mesons stemming from cosmic ray primary reactions in the upper atmosphere. Just by counting naively the neutrinos from the decay chain in Fig. 6, a ratio of $(\nu_\mu + \bar{\nu}_\mu)/(\nu_e + \bar{\nu}_e) \sim 2$ can be obtained for $E_\nu < 1$ GeV and $(\nu_\mu + \bar{\nu}_\mu)/(\nu_e + \bar{\nu}_e) \gtrsim 2$ for $E_\nu > 1$ GeV (where not all muons decay before they reach the detector).

Here the uncertainty in the flux is estimated to be $\sim 30\%$, while the uncertainty in the ratio is reduced to $\sim 5\%$. The following experimental observations provide a strong indication for neutrino oscillations:

- Reduced muon over electron neutrino ratios by almost a factor of two have been observed in the following experiments: by the Soudan2 iron calorimeter, the MACRO liquid scintillator and the IMB, Kamiokande and the high statistics Superkamiokande (Super-K) [12] Cherenkov detector experiments. (These observations solved the issue of systematic errors in Cherenkov counters caused by the fact that the early iron calorimeter experiments NUSEX and FREJUS did not observe a reduction.) The reduced ratio implies either ν_μ ($\bar{\nu}_\mu$) disappearance or ν_e ($\bar{\nu}_e$) appearance.
- The observed event rates at Super-K exhibit a zenith angle dependence. This reflects the fact that upcoming neutrinos have propagated about $\sim 10^4$ km through the earth, while neutrinos originating from the atmosphere above the detector have propagated some 10-30 km, only (see Fig. 6). The different propagation distances yield different oscillation probabilities. The measured zenith angle spectra are shown in Fig. 7.
- The first data of the long baseline accelerator experiment K2K [13] suggests confirmation of the atmospheric neutrino results.

Moreover oscillations of muon to electron neutrinos ν_e or additional “sterile” SU(2)

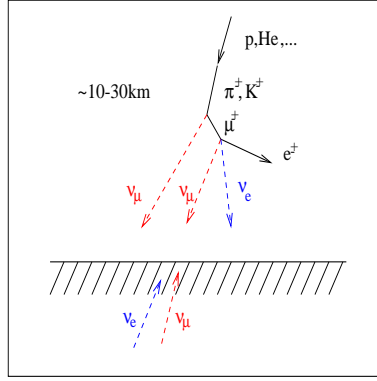


Fig. 6 Atmospheric neutrino production from π and K decays. Upward going neutrinos have propagated through the earth over a distance of about 10^4 km. This leads to enhanced oscillation probabilities as compared to neutrinos created above the detector.

singlet neutrinos ν_s can be excluded (at least to be the dominant process) from the data:

- The CHOOZ and Palo Verde reactor experiments exclude $\nu_\mu \rightarrow \nu_e$ oscillations for the parameter range of the atmospheric favored region with the non-observation of ν_e disappearance.
- In principle, sterile neutrinos imprint atmospheric data in three different ways: via differing matter effects for ν_μ oscillation to ν_τ vs. ν_s , via neutral current scattering of ν_τ but not ν_s , as measured by π^0 production; and via τ appearance from E_{ν_τ} scattering above threshold. The data show no evidence for these effects and this translates into bounds on the sterile neutrino component in atmospheric neutrinos.

In summary fits to the experimental results at different energies and zenith angles single out $\nu_\mu \rightarrow \nu_\tau$ oscillations [14] and a single region in the $\Delta m_{\text{atm}}^2 - \sin^2 2\theta_{\text{atm}}$ parameter space [1, 15], i.e. $1 \times 10^{-3} \text{ eV}^2 < \Delta m_{\text{atm}}^2 < 4 \times 10^{-3} \text{ eV}^2$, with best fit $\Delta m_{\text{atm}}^2 = 2.6 \times 10^{-3} \text{ eV}^2$, and (close to) maximal mixing $\sin^2 2\theta_{\text{atm}} > 0.7$, with best fit $\sin^2 2\theta_{\text{atm}} = 0.97$.

4.3 Solar neutrinos

Solar neutrinos are produced by the nuclear fusion reactions in the solar core. The most important neutrino sources are the reactions of the pp cycle



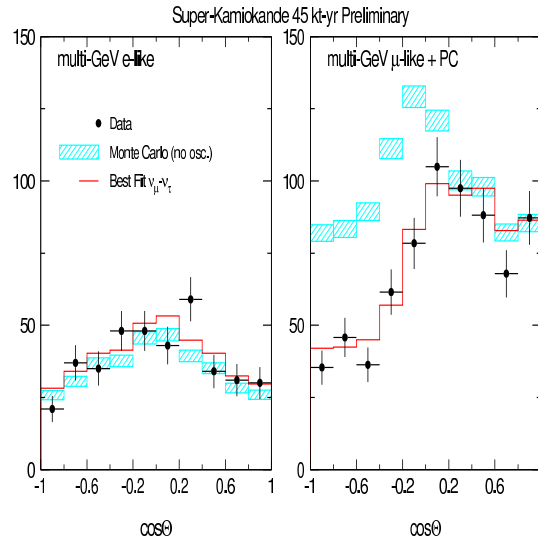


Fig. 7 Zenith angle dependence of e-like and μ -like events in Super-K. The data show a clear zenith angle dependence for μ -like events while the e-like events behave as the no-oscillation expectation [12].

which give rise to the pp , pep , ${}^7\text{Be}$ and ${}^8\text{B}$ neutrinos, respectively. A small contribution to the fluxes is produced in the CNO cycle. The corresponding energy spectra are displayed in Fig. 8, together with the sensitivities of the different experiments due to the different energy thresholds of the radiochemical Gallium (Gallex/GNO [17] and Sage [18]), Chlorine [19], and Cherenkov (Super-K [20], Kamiokande [21] and SNO [22]) detectors. Fig. 9 compares the expected (no-oscillation) neutrino fluxes with the actual measurement for the different experiments. The following conclusions can be drawn:

- All experiments observe less neutrinos than expected according to the standard solar model (SSM) [23].
- The combination of different experiments exhibits an energy dependent suppression of solar neutrino fluxes. If ${}^8\text{B}$ neutrinos are observed at Super-K and SNO, there should be pp and ${}^7\text{Be}$ neutrinos in the Gallium experiments as well. The measured rate, however, allows just for the (solar-model independent) pp neutrino flux, without any room left for contributions from ${}^7\text{Be}$ neutrinos (the absence of ${}^7\text{Be}$ neutrinos will be tested by the BOREXINO [24] experiment, which is scheduled to start taking data in 2002).
- The SNO experiment is sensitive on both neutral current (due to any neutrino flavor) and charged current (due to electron neutrinos only) reactions via the dissociation of deuterium. While the neutral current data are in perfect agreement with the fluxes predicted of the SSM, $\Phi_{NC}/\Phi_{SSM} = 1.01 \pm 0.12$, the charged

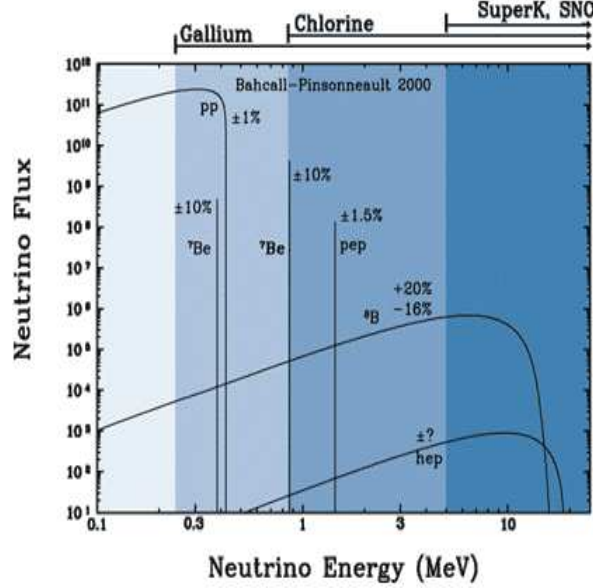


Fig. 8 Solar neutrino spectrum: Fluxes as a function of energy for the different production processes (from [16]).

current data show a suppression by roughly a factor of three. This observation can be interpreted as evidence for the appearance of solar neutrinos with a non-electron flavor.

Matter effects play a crucial role in the interpretation of the solar neutrino results. The Mikheyev-Smirnov-Wolfenstein (MSW) effect [25] is a result of different matter potentials. Larger effective masses are generated in the sun for electron neutrinos (which interact via neutral and charged current) as compared to other flavors (which interact via neutral current only).

If the (i) vacuum mass (squared) difference Δm_{\odot}^2 is not too large, a level crossing arises in the sense that the heavier mass eigenstate in the sun is the electron neutrino ν_e , while in vacuum it is mainly a different flavor ν_x .

For an (ii) adiabatic transition out of the solar core, the electron neutrino created in the sun is converted resonantly into the heavy mass eigenstate in vacuum, being mainly ν_x .

This process is especially effective for (iii) not too large mixing, since for small mixing an almost pure ν_e state is converted into an almost pure ν_x state.

The MSW conditions (i), (ii), and (iii) define isocontour lines for $P(\nu_e \rightarrow \nu_\ell)$ of triangle shape in the $\Delta m_{\odot}^2 - \sin^2 2\theta_{\odot}$ plane. The boundaries of these isocontour lines are at (i) large Δm^2 's, (ii) small Δm^2 combined with small mixing angles and (iii) large mixing angles. Since any experiment gives a range of probabilities because of finite error bars, the allowed regions are bands, whose limiting curves have the shape of a triangle. The superposition of the bands corresponding to different experiments

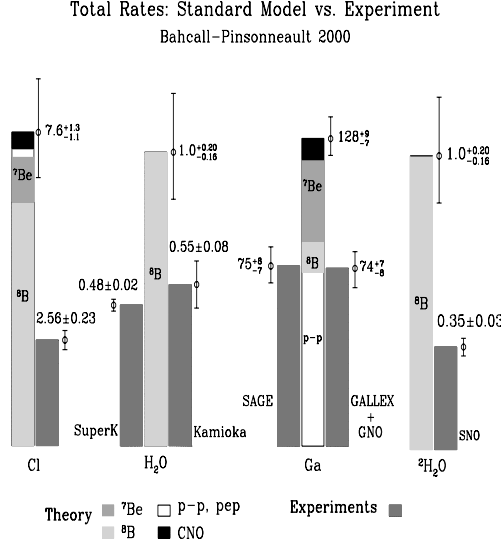


Fig. 9 Measured rates of neutrino experiments versus expectations in the solar standard model (from [16]).

defines through the overlap favored regions usually known as the small (SMA) and large (LMA) mixing angle MSW solutions.

The SMA solution has been disfavored by the flat energy spectrum measured at Super-K. After the release of the SNO data, the LMA solution is selected at a 99 % confidence level (C.L.) and is also favored if one only analyzes the total rates. Also solutions with $\theta_\odot \geq \pi/4$ have been excluded. Thus the solution to the solar neutrino problem can be summarized as [26] $\nu_e \rightarrow \nu_{\mu,\tau}$ oscillations with $2.7 \times 10^{-5} \text{ eV}^2 < \Delta m_\odot^2 < 1.8 \times 10^{-4} \text{ eV}^2$, with best fit $\Delta m_\odot^2 = 5.6 \times 10^{-5} \text{ eV}^2$, and $0.27 < \tan^2 \theta_\odot < 0.55$, with best fit $\tan^2 \theta_\odot = 0.39$. It has become customary to express a mixing angle sensitive to matter effects, such as the solar angle, as $\tan \theta$ rather than $\sin 2\theta$ in order to account for the octant of the “dark side”, $\pi/4 < \theta \leq \pi/2$.

Limits on the solar mode $\nu_e \rightarrow \nu_s$ result from model fits to the Super-K solar data, but especially from the recent SNO data. There is no evidence favoring a sterile admixture in the neutrino flux from the sun. Nevertheless, a large sterile component remains compatible with the SNO result, because of the uncertainty in the true high-energy solar neutrino flux produced by the ^8B reaction in the sun.

4.4 LSND and a 4th sterile neutrino?

A third experimental evidence has been reported by the LSND experiment [27]. LSND was searching for $\bar{\nu}_\mu \rightarrow \bar{\nu}_e$ and $\nu_\mu \rightarrow \nu_e$ appearance from the products of pion and subsequent muon decay, produced by the scattering of accelerated protons on a fixed

target:

$$\begin{aligned}
 p + \text{target} &\rightarrow \pi^+ + X, \\
 \pi^+ &\rightarrow \mu^+ \nu_\mu \quad (\text{decay in flight}), \\
 \mu^+ &\rightarrow e^+ \nu_e \bar{\nu}_\mu \quad (\text{decay at rest}).
 \end{aligned} \tag{19}$$

LSND has observed a clear excess of events with $\bar{\nu}_e$ signature, which has been interpreted as evidence for neutrino oscillations with $P(\bar{\nu}_\mu \rightarrow \bar{\nu}_e) = 0.31\% (+0.11\% \pm 0.05\%)$. In addition an analysis of $\nu_\mu \rightarrow \nu_e$ oscillations from the decay in flight has been performed and an oscillation probability of $P(\nu_\mu \rightarrow \nu_e) = 0.26\% (\pm 0.07\% \pm 0.05\%)$ has been deduced, being consistent with the $\bar{\nu}_\mu \rightarrow \bar{\nu}_e$ results. The favored regions are constrained by the negative result of the KARMEN experiment, which is similar to LSND but possesses a smaller baseline. A combined analysis favors $\nu_\mu \rightarrow \nu_e$ oscillations with $0.12 \text{ eV}^2 < \Delta m_{\text{LSND}}^2 < 1.1 \text{ eV}^2$ and $10^{-3} < \sin^2 2\theta_{\text{LSND}} < 0.7$.

Taken at face value, the solar, atmospheric, and LSND data require three independent Δm^2 scales. Thus, four neutrinos seem to be required. The Z-boson width further requires that one of these four neutrinos be a “sterile” $SU(2) \times U(1)$ electroweak-singlet. In the so-called 2+2 spectrum, the LSND scale splits two pairs of neutrino mass-eigenstates. Phenomenologically, it is required that one pair mix ν_μ with ν_τ and ν_s for explaining the atmospheric ν_μ disappearance, while the second pair mix ν_e with ν_τ and ν_s for explaining the solar ν_e disappearance. The small LSND amplitude is accommodated with a small mixing of ν_e into the first pair, and a small mixing of ν_μ into the second pair.

A sum rule requires a robust contribution of $\nu_\mu \rightarrow \nu_s$ in the atmospheric data and/or $\nu_e \rightarrow \nu_s$ in the solar data. The essence of the sum rule is that the sterile neutrino may hide from solar oscillations, or from atmospheric oscillations, but cannot hide from both [28]. When the small angles, which mix the neutrinos in the atmospheric pair with the ones in the solar pair, are neglected, the sum rule states that the probabilities to produce ν_s in the solar and in the atmospheric data sum to unity:

$$\left[\frac{P(\nu_e \rightarrow \nu_s)}{P(\nu_e \rightarrow \nu_\ell)} \right]_{\text{sun}} + \left[\frac{P(\nu_\mu \rightarrow \nu_s)}{P(\nu_\mu \rightarrow \nu_\mu)} \right]_{\text{atm}} = 1. \tag{20}$$

The relaxation of this sum rule, when matter effects and small angles are included, has been studied in [29] taking into account the bounds on ν_s admixture in solar and atmospheric neutrinos [30]. In Fig. 10 the approximate sum rule is analyzed in generality, varying the usually neglected mixing angles in their experimentally allowed ranges including possible matter effects. The strong bound from atmospheric neutrinos is barely consistent with the 2+2 scheme, when 90 % C.L. bounds are applied. At 99 % C.L., though, the 2+2 four neutrino scheme with sterile neutrinos is still allowed (compare also the fit results in [30]). The neutrino oscillation solution to LSND experiment will definitely be tested soon by the accelerator experiment MiniBooNE, which has an improved background and a significant larger baseline.

An interesting and elegant alternative to an oscillation solution for LSND is provided by lepton number violating anomalous muon decays,

$$\mu^+ \rightarrow e^+ \bar{\nu}_e \bar{\nu}_i, \tag{21}$$

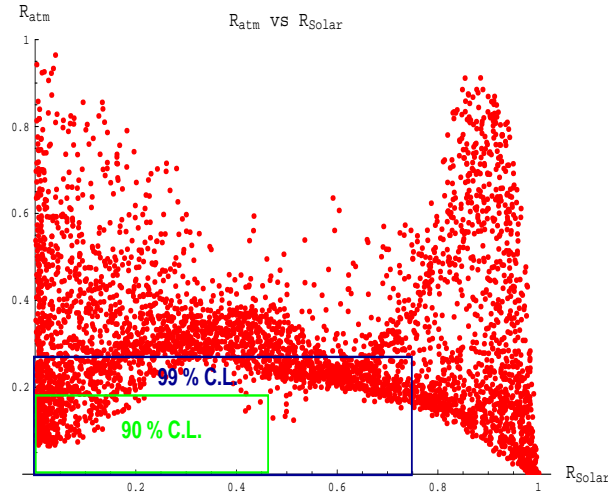


Fig. 10 Sum rule for sterile neutrinos. The scatter points correspond to allowed values of small mixing angles. Also shown are the allowed regions for ν_s admixture in solar and atmospheric neutrinos at 90 % C.L. and 99 % C.L. (from [29]).

which does not require sterile neutrinos and not necessarily predicts a MiniBooNE signal [32].

4.5 Neutrino Oscillation Summary

Over the past years a unique picture of neutrino mixing has been evolved, see Fig. 11. The bounds on sterile neutrinos from solar and atmospheric neutrino data suggest strongly a three neutrino framework. Large/maximal mixing has been established for solar and atmospheric neutrinos, respectively, and the third mixing angle is strongly bounded by reactor neutrino experiments. The neutrino mixing matrix, modulo CP violating phases, turns out to be of the following approximate form [33]:

$$U = \begin{pmatrix} \cos \theta_\odot & \sin \theta_\odot & 0 \\ -\frac{\sin \theta_\odot}{\sqrt{2}} & \frac{\cos \theta_\odot}{\sqrt{2}} & \frac{1}{\sqrt{2}} \\ \frac{\sin \theta_\odot}{\sqrt{2}} & -\frac{\cos \theta_\odot}{\sqrt{2}} & \frac{1}{\sqrt{2}} \end{pmatrix} \approx \begin{pmatrix} \frac{1}{\sqrt{2}} & \frac{1}{\sqrt{2}} & 0 \\ -\frac{1}{2} & \frac{1}{2} & \frac{1}{\sqrt{2}} \\ \frac{1}{2} & -\frac{1}{2} & \frac{1}{\sqrt{2}} \end{pmatrix} \quad (22)$$

In addition, the mass squared differences $\Delta m_\odot^2 \simeq 6 \times 10^{-5} \text{ eV}^2$ and $\Delta m_{\text{atm}}^2 \simeq 3 \times 10^{-3} \text{ eV}^2$ are known. Future neutrino oscillation experiments will increase the accuracy of these parameters as follows:

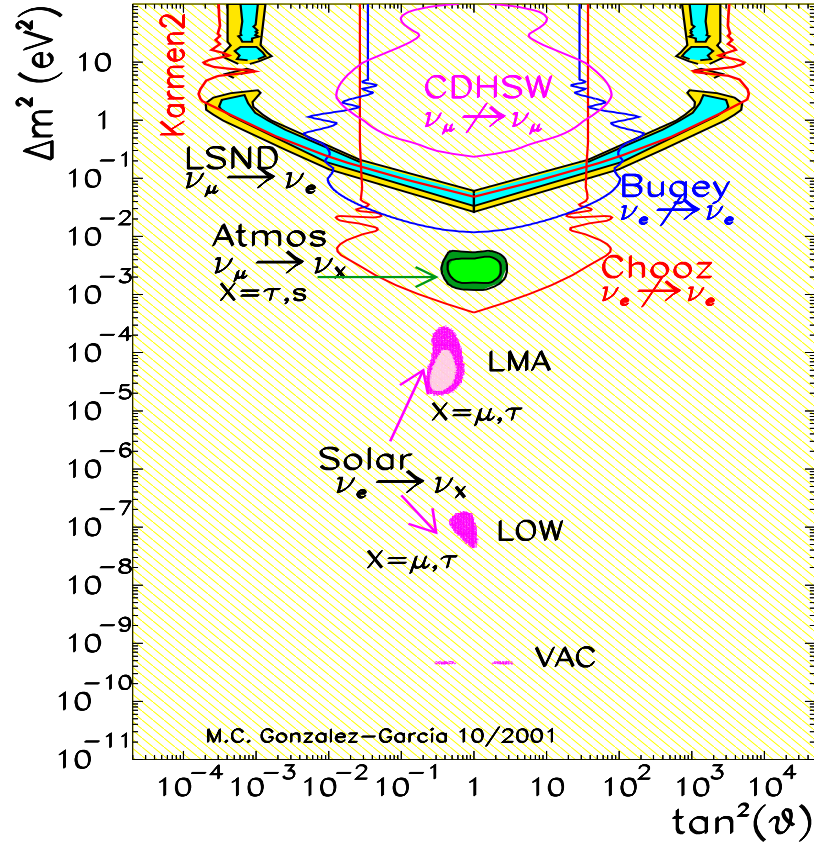


Fig. 11 Summary of evidences for neutrino oscillations (from [1]).

- Δm_{\odot}^2 and $\sin^2 2\theta_{\odot}$: The long-baseline reactor experiment KamLAND is designed to test the LMA MSW solution of the solar neutrino problem. Data taking has been started in 2002 and the solar neutrino parameters will be determined with an accuracy of $\delta(\Delta m_{\odot}^2)/\Delta m_{\odot}^2 = 10\%$ and $\delta(\sin^2 2\theta_{\odot}) = \pm 0.1$ within three years of measurement [34].
- Δm_{atm}^2 and $\sin^2 2\theta_{\text{atm}}$: The atmospheric oscillation parameters will be determined by the long-baseline accelerator experiment MINOS with an accuracy of $\delta(\Delta m_{\text{atm}}^2)/\Delta m_{\text{atm}}^2 = 30\%$ and $\delta(\sin^2 2\theta_{\text{atm}}) = \pm 0.1$ [35].
- $\sin^2 2\theta_{13}$: The long baseline experiment MINOS [35] has a sensitivity down to $\sin^2 2\theta_{13} < 0.02$ - 0.05 . A future neutrino factory [36] or the analysis of the neutrino energy spectra of a future galactic supernova [37] may provide a sensitivity down to 10^{-4} .
- *Direct/inverse type of hierarchy*: The inverse hierarchical spectrum with two heavy and a single light state is disfavored according to a recent analysis [38] of the neutrino spectrum from supernova SN1987A, unless the mixing angle θ_{13} is large (compare, however, [39]).

Nothing is known so far about the remaining parameters, the three CP violating phases (one Dirac and two Majorana phases) and the absolute neutrino mass scale.

- At a neutrino factory one may be able to distinguish $\delta = 0$ from $\pi/2$ if $\Delta m_{\odot}^2 > 10^{-5} \text{ eV}^2$ [40].
- Even more difficult is the determination of Majorana phases, some information might be obtained by comparing positive results in future double beta decay and tritium beta decay experiments [41] or by testing related sneutrino mass matrices in supersymmetric theories.

Especially important for obtaining information on the theoretical structures underlying the SM of particle physics is the full reconstruction of the neutrino mass spectrum and thus the determination of the absolute neutrino mass. The rest of this review concentrates on this difficult task.

5 Absolute neutrino masses: direct determination

While neutrino oscillation experiments provide information on the neutrino mass squared differences Δm_{ij}^2 , the absolute scale of the neutrino masses is not known so far. Upper bounds can be obtained from the neutrino hot dark matter contribution to the cosmological large scale structure evolution and the Cosmic Microwave Background, from the interpretation of the extreme energy cosmic rays in the Z-burst model, from tritium beta decay experiments, and, most importantly, from neutrinoless double beta decay experiments [3].

5.1 Tritium beta decay

In tritium decay, the larger the mass states comprising $\bar{\nu}_e$, the smaller is the Q-value of the decay. The manifestation of neutrino mass is a reduction of phase space for the produced electron at the high energy end of its spectrum. An expansion of the decay rate formula about m_{ν_e} leads to the end point sensitive factor

$$m_{\nu_e}^2 \equiv \sum_j |U_{ej}|^2 m_j^2, \quad (23)$$

where the sum is over mass states which can kinematically alter the end-point spectrum. If the neutrino masses are nearly degenerate, then unitarity of U leads immediately to a bound on the heaviest neutrino mass eigenstate $\sqrt{m_{\nu_e}^2} = m_3$. The design of a larger tritium decay experiment (KATRIN) for improving the present 2.2 eV m_{ν_e} bound is under discussion; direct mass limits as low as 0.4 eV, or even 0.2 eV, may be possible in this type of experiment [42].

5.2 CMB/LSS cosmological limits

According to Big Bang cosmology, the masses of nonrelativistic neutrinos are related to the neutrino fraction of closure density by $\sum_j m_j = 40 \Omega_\nu h_{65}^2$ eV, where h_{65} is the present Hubble parameter in units of 65 km/(s Mpc). As knowledge of large-scale structure (LSS) formation has evolved, so have the theoretically preferred values for the hot dark matter (HDM) component, Ω_ν . In fact, the values have declined. In the once popular HDM cosmology, one had $\Omega_\nu \sim 1$ and $m_\nu \sim 10$ eV for each of the mass-degenerate neutrinos. In the cold-hot CHDM cosmology, the cold matter was dominant and one had $\Omega_\nu \sim 0.3$ and $m_\nu \sim 4$ eV for each neutrino mass. In the currently favored Λ CDM cosmology with a non-vanishing cosmological constant Λ , there is scant room left for the neutrino component. The power spectrum of early-Universe density perturbations is processed by gravitational instabilities. However, the free-streaming relativistic neutrinos suppress the growth of fluctuations on scales below the horizon (approximately the Hubble size $c/H(z)$) until they become nonrelativistic at redshifts $z \sim m_j/3T_0 \sim 1000 (m_j/\text{eV})$.

A recent limit [43] derived from the power spectrum obtained in the 2dF (Two Degree Field system) Galaxy Redshift Survey constrains the fractional contribution of massive neutrinos to the total mass density to be less than 0.13 (for a total matter mass density $0.1 < \Omega_m < 0.5$ and a scalar spectral index $n = 1$). This translates into a bound on the sum of neutrino mass eigenvalues, $\sum_j m_j < 1.8$ eV. Previous cosmological bounds from the data of galaxy cluster abundances, the Lyman α forest and data compilations including the cosmic microwave background (CMB), peculiar velocities and large scale structure give upper bounds on the sum of neutrino masses in the range 3-6 eV (see also [44]). It was estimated in [45] that the precision determination of the power spectrum shape by the Sloan Digital Sky Survey, combined with the CMB data of the MAP satellite experiment can reach a sensitivity of $\sum m_\nu \lesssim 0.65$ eV. For discussions of possible limits from future time of flight measurements of supernova or gamma ray burst neutrinos see [46].

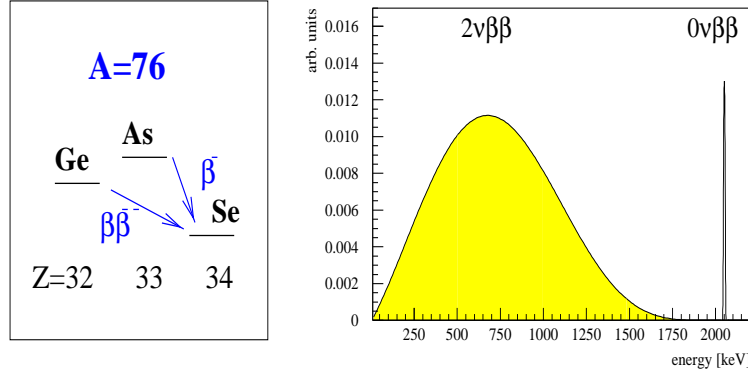


Fig. 12 Left panel: Nuclear spectrum allowing for observable double beta decay. Right panel: Energy spectrum for the SM allowed $2\nu\beta\beta$ decay and $0\nu\beta\beta$ decay: the sharp peak at the Q-value provides a clear signature for non-vanishing neutrino masses

Some caution is warranted in the cosmological approach to neutrino mass in that the many cosmological parameters may conspire in various combinations to yield nearly identical CMB and LSS data. An assortment of very detailed data may be needed to resolve the possible “cosmic ambiguities”.

6 Neutrinoless double beta decay

The $0\nu\beta\beta$ [47] process corresponds to two single beta decays occurring simultaneously in one nucleus and converts a nucleus (Z,A) into a nucleus $(Z+2,A)$, see Fig. 12. The SM allowed process emitting two antineutrinos,

$${}^A_Z X \rightarrow {}^A_{Z+2} X + 2e^- + 2\bar{\nu}_e, \quad (24)$$

is one of the rarest processes in nature with half lives in the region of 10^{21-24} years. More interesting is the search for the neutrinoless mode,

$${}^A_Z X \rightarrow {}^A_{Z+2} X + 2e^- \quad (25)$$

which violates lepton number by two units and thus implies physics beyond the SM.

The $0\nu\beta\beta$ rate is a sensitive tool for the measurement of the absolute mass-scale for Majorana neutrinos [48]. The observable measured in the amplitude of $0\nu\beta\beta$ is the ee element of the neutrino mass-matrix in the flavor basis (see Fig. 13). Expressed in terms of the mass eigenvalues and neutrino mixing-matrix elements, it is

$$m_{ee} = \left| \sum_i U_{ei}^2 m_i \right|. \quad (26)$$

A reach to a value as low as $m_{ee} \sim 0.01$ eV seems possible with proposed double beta decay projects such as GENIUSI, MAJORANA, EXO, XMASS or MOON. This

provides a substantial improvement over the current bound of $m_{ee} < 0.6$ eV. A recent report [49] of the Heidelberg-Moscow experiment claims a best fit value of $m_{ee} = 0.36$ eV, but it is subject to controversions regarding the background determination. In the far future, another order of magnitude in reach is available to the 10 ton version of GENIUS, provided it will be funded and commissioned.

For masses in the interesting range $\gtrsim 0.01$ eV, the two light mass eigenstates are nearly degenerate and hence the approximation $m_1 = m_2$ (partial or total degeneracy) is justified. Due to the restrictive CHOOZ bound, $|U_{e3}|^2 < 0.025$, the contribution of the third mass eigenstate is nearly decoupled from m_{ee} and hence $U_{e3}^2 m_3$ may be neglected in the $0\nu\beta\beta$ formula. We label by ϕ_{12} the relative phase between $U_{e1}^2 m_1$ and $U_{e2}^2 m_2$. Then, employing the above approximations, we arrive at a very simplified expression for m_{ee} :

$$m_{ee}^2 = \left[1 - \sin^2(2\theta_\odot) \sin^2\left(\frac{\phi_{12}}{2}\right) \right] m_1^2. \quad (27)$$

The two CP-conserving values of ϕ_{12} are 0 and π . These same two values give maximal constructive and destructive interference of the two dominant terms in eq. (26), which leads to upper and lower bounds for the observable m_{ee} in terms of a fixed value of m_1 :

$$\cos(2\theta_\odot) m_1 \leq m_{ee} \leq m_1, \quad \text{for fixed } m_1. \quad (28)$$

The upper bound becomes an equality, $m_{ee} = m_1$, if $\phi_{12} = 0$. The lower bound depends on Nature's value of the mixing angle in the LMA solution. A consequence of eq. (28) is that for a given measurement of m_{ee} , the corresponding inference of m_1 is uncertain over the range $[m_{ee}, m_{ee} \cos(2\theta_\odot)]$ due to the unknown phase difference ϕ_{12} , with $\cos(2\theta_\odot) > 0.1$ [26]. This uncertainty disfavors $0\nu\beta\beta$ in comparison to direct measurements if a specific value of m_1 has to be determined, while $0\nu\beta\beta$ is more sensitive as long as bounds on m_1 are aimed at. Knowing the value of θ_\odot better will improve the estimate of the inherent uncertainty in m_1 . The forthcoming KamLAND experiment should reduce the error in the mixing angle.

A far future 10 ton version of GENIUS would be sensitive even to hierarchical neutrino spectra, $m_1 \simeq 0 \ll m_2 \ll m_3$. A summary of the aimed sensitivities of future $0\nu\beta\beta$ projects to different neutrino spectra is given in Fig. 14 including the inverse hierarchy, in which the ν_e admixture is mainly in the heaviest state.

7 Extreme energy cosmic rays in the Z-burst model

It was expected that the extreme energy cosmic ray (EECR) primaries would be protons from outside of our Galaxy, produced in Nature's most extreme environments such as the tori or radio hot spots of active galactic nuclei (AGN). Indeed, cosmic ray data show a spectral flattening just below 10^{19} eV which can be interpreted as a new extragalactic component overtaking the lower energy galactic component; the energy of the break correlates well with the onset of a Larmor radius for protons too large to be contained by the Galactic magnetic field. It was further expected that the extragalactic spectrum would reveal an end at the Greisen-Kuzmin-Zatsepin (GZK)

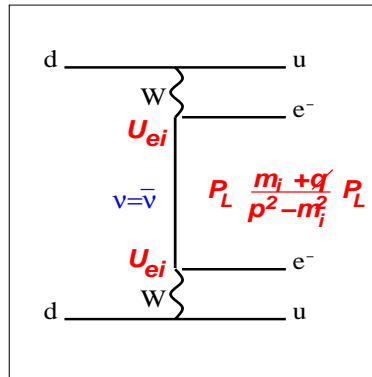


Fig. 13 Diagram for neutrinoless double beta decay.

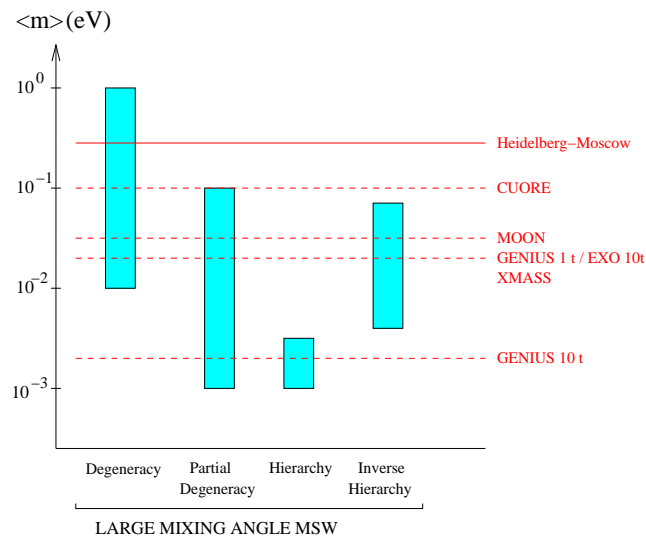


Fig. 14 Different neutrino mass spectra versus sensitivities of future double beta decay projects. A futuristic 10 ton Genius experiment may test all neutrino spectra.

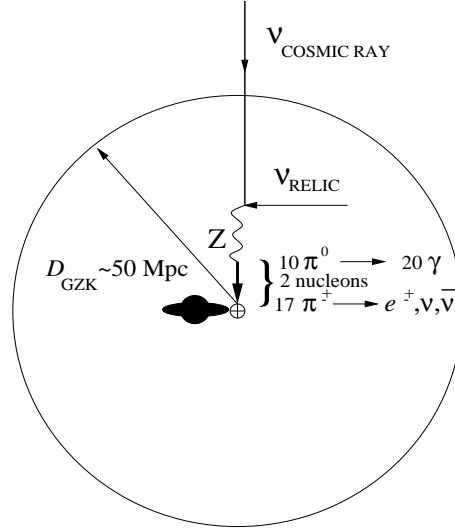


Fig. 15 Schematic diagram showing the production of a Z-burst resulting from the resonant annihilation of a cosmic ray neutrino on a relic (anti)neutrino. If the Z-burst occurs within the GZK zone (~ 50 to 100 Mpc) and is directed towards the earth, then photons and nucleons with energy above the GZK cutoff may arrive at earth and initiate super-GZK air-showers.

cutoff energy of $E_{\text{GZK}} \sim 5 \times 10^{19}$ eV. The origin of the GZK cutoff is the degradation of nucleon energy by the resonant scattering process $N + \gamma_{2.7K} \rightarrow \Delta^* \rightarrow N + \pi$ when the nucleon is above the resonant threshold E_{GZK} . The concomitant energy-loss factor is $\sim (0.8)^{D/6\text{Mpc}}$ for a nucleon traversing a distance D . Since no AGN-like sources are known to exist within 100 Mpc of the earth, the energy requirement for a proton arriving at the earth with a super-GZK energy is unrealistically high. Nevertheless, to date more than twenty events with energies at and above 10^{20} eV have been observed (for recent reviews see [50]).

Several solutions have been proposed for the origin of these EECRs, ranging from unseen Zevatron accelerators ($1 \text{ ZeV} = 10^{21}$ eV) and decaying supermassive particles and topological defects in the Galactic vicinity, to exotic primaries, exotic new interactions, and even exotic breakdown of conventional physical laws. A rather conservative and economical scenario involves cosmic ray neutrinos which scatter resonantly at the cosmic neutrino background (CNB) predicted by Standard Cosmology and produce Z-bosons [51]. These Z-bosons in turn decay to produce a highly boosted “Z-burst”, containing on average twenty photons and two nucleons above E_{GZK} (see Fig. 15). The photons and nucleons from Z-bursts produced within a distance of 50 to 100 Mpc of the earth can reach the earth with enough energy to initiate the air-showers observed at $\sim 10^{20}$ eV.

The energy of the neutrino annihilating at the peak of the Z-pole is

$$E_{\nu_j}^R = \frac{M_Z^2}{2m_j} = 4 \left(\frac{\text{eV}}{m_j} \right) \text{ZeV}. \quad (29)$$

Even allowing for energy fluctuations about mean values, it is clear that in the Z-burst model the relevant neutrino mass cannot exceed ~ 1 eV. On the other hand, the neutrino mass cannot be too light. Otherwise the predicted primary energies will exceed the observed event energies and the primary neutrino flux will be pushed to unattractively higher energies. In this way, one obtains a rough lower limit on the neutrino mass of ~ 0.1 eV for the Z-burst model (with allowance made for an order of magnitude energy-loss for those secondaries traversing 50 to 100 Mpc). A detailed comparison of the predicted proton spectrum with the observed EECR spectrum in [52] yields a value of $m_\nu = 0.26_{-0.14}^{+0.20}$ eV for extragalactic halo origin of the power-like part of the spectrum.

A necessary condition for the viability of this model is a sufficient flux of neutrinos at $\gtrsim 10^{21}$ eV. Since this condition seems challenging, any increase of the Z-burst rate is helpful, that ameliorates slightly the formidable flux requirement. If the neutrinos are mass degenerate, then a further consequence is that the Z-burst rate at E_R is three times what it would be without degeneracy. If the neutrino is a Majorana particle, a factor of two more is gained in the Z-burst rate relative to the Dirac neutrino case since the two active helicity states of the relativistic CNB depolarize upon cooling to populate all spin states.

Moreover the viability of the Z-burst model is enhanced if the CNB neutrinos cluster in our matter-rich vicinity of the universe. For smaller scales, the Pauli blocking of identical neutrinos sets a limit on density enhancement. As a crude estimate of Pauli blocking, one may use the zero temperature Fermi gas as a model of the gravitationally bound neutrinos. Requiring that the Fermi momentum of the neutrinos does not exceed the mass times the virial velocity $\sigma \sim \sqrt{MG/L}$ within the cluster of mass M and size L , one gets the Tremaine-Gunn bound

$$\frac{n_{\nu_j}}{54 \text{ cm}^{-3}} \lesssim 10^3 \left(\frac{m_j}{\text{eV}} \right)^3 \left(\frac{\sigma}{200 \text{ km/s}} \right)^3. \quad (30)$$

With a virial velocity within our Galactic halo of a couple hundred km/s, it appears that Pauli blocking allows significant clustering on the scale of our Galactic halo only if $m_j \gtrsim 0.5$ eV. Free-streaming (not considered here) also works against HDM clustering.

Thus, if the Z-burst model turns out to be the correct explanation of EECRs, then it is probable that neutrinos possess one or more masses in the range $m_\nu \sim (0.1-1)$ eV. Mass-degenerate neutrino models are then likely. Some consequences are:

- A value of $m_{ee} > 0.01$ eV, and thus a signal of $0\nu\beta\beta$ in next generation experiments, assuming the neutrinos are Majorana particles.
- Neutrino mass sufficiently large to affect the CMB/LSS power spectrum.

8 Conclusions

Solar and atmospheric neutrino oscillations have established solid evidence for non-vanishing neutrino masses. A unique picture of the mixing matrix U and mass squared differences in a three neutrino framework is evolving with increasing accuracy. Massive neutrinos also can provide information about the theoretical structures underlying the standard model and may well be a key to the physics of supersymmetry, grand unification or extra dimensions. A crucial if not the most important parameter in this context is the absolute neutrino mass scale. Information about absolute neutrino masses can be obtained from direct determinations via tritium beta decay or cosmology. More sensitive in giving limits but less valuable for determining the mass scale is neutrinoless double beta decay. The most ambitious proposals for future double beta decay experiments, such as the 10 ton version of GENIUS, may in fact test all possible neutrino mass spectra. The puzzle of EECRs above the GZK cutoff can be solved conservatively with the Z-burst model, connecting the ZeV scale of EECRs to the sub-eV scale of neutrino masses. If the Z-burst model turns out to be correct, neutrino masses in the region of 0.1-1 eV are predicted and degenerate scenarios are favored. In this case positive signals for future tritium beta decay experiments, CMB/LSS studies, and next-generation $0\nu\beta\beta$ experiments can be expected.

Acknowledgements

I would like to thank E. Müller-Hartmann and R. Schmitz for the kind invitation to give a colloquium talk at the University of Köln this review is based on. This work was supported by the Bundesministerium für Bildung und Forschung (BMBF, Bonn, Germany) under the contract number 05HT1WWA2.

References

- [1] M.C. Gonzalez-Garcia, Y. Nir, hep-ph/0202058.
- [2] J.W.F. Valle, hep-ph/0205216, Proc. DARK2002, February 4-9, 2002, Cape Town, South Africa; S.M. Bilenky, C. Giunti, W. Grimus, Prog. Part. Nucl. Phys. **43** (1999) 1-86; G. Altarelli, F. Feruglio, hep-ph/0206077, to appear in "Neutrino Mass", Springer Tracts in Modern Physics; E. Kh. Akhmedov, hep-ph/0001264, Lectures given at Trieste Summer School in Particle Physics, June 7 – July 9, Italy; R.N. Mohapatra, Nucl. Phys. Proc. Suppl. **91** (2001) 313-320.
- [3] H. Päs, T.J. Weiler, Phys. Rev. **D 63** (2001) 113015
- [4] M. Gell-Mann, P. Ramond and R. Slansky, Proc. Supergravity Stony Brook Workshop, New York 1979, eds. P. Van Nieuwenhuizen and D. Freedman; T. Yanagida, Proc. Workshop on Unified Theories and Baryon Number in the Universe, Tsukuba, Japan 1979, eds. A. Sawada and A. Sugamoto; R. N. Mohapatra and G. Senjanovic, Phys. Rev. Lett. **44**, 912 (1980), *erratum* Phys. Rev. **D 23**, 165 (1993).
- [5] J. Hisano and D. Nomura, Phys. Rev. **D 59** (1999) 116005
- [6] F. Deppisch, H. Päs, A. Redelbach, R. Rückl, Y. Shimizu, hep-ph/0206122, and references therein.
- [7] S. Dimopoulos, L. Hall, Phys. Lett. **B 207** (1987) 210; R. Godbole, P. Roy, X. Tata, Nucl. Phys. **B 401** (1993) 67; M.A. Diaz, J.C. Romao, J.W.F. Valle, Nucl. Phys. **B 524** (1998) 23.

- [8] G. Bhattacharyya, H.V. Klapdor-Kleingrothaus, H. Päs, Phys. Lett. **B 463** (1999) 77, and references therein.
- [9] N. Arkani-Hamed, S. Dimopoulos, G.R. Dvali, J. March-Russell, Phys. Rev. **D 65** (2002) 024032; K.R. Dienes, E. Dudas, T. Gherghetta, Nucl. Phys. **B 557** (1999) 25; Y. Grossman, M. Neubert, Phys. Lett. **B 474** (2000) 361-371; S.J. Huber, Q. Shafi, hep-ph/0205327.
- [10] M. Apollonio *et al.* [CHOOZ Collaboration], Phys. Lett. **B 466** (1999) 415.
- [11] F. Boehm *et al.*, Phys. Rev. **D 64** (2001) 112001.
- [12] Y. Fukuda *et al.* [SuperKamiokande Collaboration], Phys. Rev. Lett. **81** (1998) 1562; Phys. Rev. Lett. **82** (1999) 2644. Y. Fukuda *et al.*, Phys. Lett. **B 433**, 9 (1998); Phys. Lett. **B 436**, 33 (1998);
- [13] K. Nishikawa *et al.* (K2K Collab.), Proc. of the EPS HEP 2001 conference, July 12-18, 2001, Budapest, Hungary.
- [14] J.G. Learned, S. Pakvasa, T.J. Weiler, Phys. Lett. **B 207** (1988) 79.
- [15] N. Fornengo, M.C. Gonzalez-Garcia, J. W. F. Valle, Nucl. Phys. **B 580** (2000) 58-82; G.L. Fogli, E. Lisi, A. Marrone, D. Montanino, Nucl. Phys. Proc. Suppl. **91** (2001) 167-173.
- [16] J.N. Bahcall website, <http://www.sns.ias.edu/~jnb/>
- [17] GALLEX Collaboration, W. Hampel *et al.*, Phys. Lett. **B 447** (1999) 127 .
- [18] SAGE Collaboration, J.N. Abdurashitov *et al.*, Phys. Rev. **C 60** (1999) 055801; V. Gavrin, Nucl. Phys. Proc. Suppl. **91** (2001) 36.
- [19] Homestake Collaboration, B.T. Cleveland *et al.*, Astrophys. J. **496** (1998) 505; R. Davis, Prog. Part. Nucl. Phys. **32** (1994) 13; K. Lande, Nucl. Phys. Proc. Suppl. **77** (1999) 13.
- [20] S. Fukuda *et al.*, (SuperKamiokande Collab.) Phys. Rev. Lett. **86** (2001) 5651.
- [21] Y. Fukuda *et al.* (Kamiokande Collab.), Phys. Rev. Lett. **77** (1996) 1683
- [22] Q.R. Ahmad *et al.* (SNO Collab.), Phys. Rev. Lett. **89** (2002) 011301; Q.R. Ahmad *et al.* (SNO Collab.), Phys. Rev. Lett. **87** (2001) 071301.
- [23] J.N. Bahcall, M.H. Pinsonneault, S. Basu Astrophys. J. **555** (2001) 990-1012.
- [24] L. Oberauer, Nucl. Phys. Proc. Suppl. **77** (1999) 48.
- [25] L. Wolfenstein, Phys. Rev. **D 17** (1978) 2369; S.P. Mikheyev, A.Y. Smirnov, Sov. J. Nucl. Phys. **42** (1985) 913
- [26] V. Barger, D. Marfatia, K. Whisnant, B. P. Wood, hep-ph/0204253, J.N. Bahcall, M.C. Gonzalez-Garcia, C. Pena-Garay, JHEP **0108** (2001) 014; A. Bandyopadhyay, S. Choubey, S. Goswami, D.P. Roy, Phys. Lett. **B 540** (2002) 14-19.
- [27] C. Athanassopoulos *et al.* (LSND Collab.), Phys. Rev. Lett. **77** (1996) 3082-3085; Phys. Rev. Lett. **81** (1998) 1774-1777; K. Eitel, New Jour.Phys. **2** (2000) 1.
- [28] O. L. Peres, A. Y. Smirnov, Nucl. Phys. **B 599** (2001) 3.
- [29] H. Päs, L. Song, T.J. Weiler, hep-ph/0209373.
- [30] M.C. Gonzalez-Garcia, M. Maltoni, C. Pena-Garay, Phys. Rev. **D 64** (2001) 093001; hep-ph/0108073; M. Maltoni, T. Schwetz, J.W.F. Valle, Phys. Rev. **D 65** (2002) 093004.
- [31] R. Stefanski *et al.* (MiniBooNE Collab.) Nucl. Phys. Proc. Suppl. **110** (2002) 420-422.
- [32] S. Bergmann, H.V. Klapdor-Kleingrothaus, H. Päs, Phys. Rev. **D 59** (2000) 093005; K.S. Babu, S. Pakvasa, hep-ph/0204236; see also: S. Pakvasa, Pramana **54** (2000) 65; P. Herczeg, Proc. Beyond the Desert, , June 8-14 1999, Castle Ringberg, Germany.
- [33] V. D. Barger, S. Pakvasa, T. J. Weiler and K. Whisnant, Phys. Lett. **B 437** (1998) 107.
- [34] V. Barger, D. Marfatia, B. P. Wood, Phys. Lett. **B 498**, 53 (2001); H. Murayama, A. Pierce, Phys. Rev. **D 65** (2002) 013012.
- [35] MINOS Technical Design Report, http://www.hep.anl.gov/ndk/hypertext/minos_tdr.html.
- [36] V. Barger, hep-ph/0102052.
- [37] A. S. Dighe, A. Y. Smirnov, Phys. Rev. **D 62**, 033007 (2000).
- [38] H. Minakata, H. Nunokawa, Phys. Lett. **B 504**, 301 (2001); C. Lunardini, A. Y. Smirnov, Phys. Rev. **D 63**, 073009 (2001).
- [39] V. Barger, D. Marfatia, B. P. Wood, Phys. Lett. **B 532** (2002) 19-28.
- [40] J. J. Gomez-Cadenas, Nucl. Phys. Proc. Suppl. **99B**, 304 (2001).

- [41] S. Pascoli, S. T. Petcov, L. Wolfenstein, Phys. Lett. **B 524** (2002) 319-331; W. Rodejohann, hep-ph/0203214; M. Frigerio, A.Yu. Smirnov, hep-ph/0202247; K. Matsuda, T. Kikuchi, T. Fukuyama, H. Nishiura, hep-ph/0204254; V. Barger, S.L. Glashow, P. Langacker, D. Marfatia, hep-ph/0205290, H. Nunokawa, W.J.C. Teves, R. Zukanovich Funchal, hep-ph/0206137.
- [42] C. Weinheimer, Nucl. Phys. Proc. Suppl. **91** (2001) 273-279; A. Osipowicz *et al.*, (KATRIN Collab.), hep-ex/0101091.
- [43] Ø. Elgarøy *et al.* (2dF Collab.) astro-ph/0204152.
- [44] S. Hannestad, astro-ph/0205223.
- [45] W. Hu, D.J. Eisenstein, M. Tegmark, Phys. Rev. Lett. **80** (1998) 5255.
- [46] J. Beacom, R. Boyd, A. Mezzacappa, Phys. Rev. Lett. **85** (2000) 3568; S. Choubey, S.F. King, hep-ph/0207260.
- [47] S.R. Elliott, P. Vogel, hep-ph/0202264; H.V. Klapdor-Kleingrothaus, H. Päs, hep-ph/0002109, in: Proc. of the *International Workshop on Particle Physics and the Early Universe*, September 27 - October 2, 1999, Trieste, Italy.
- [48] H.V. Klapdor-Kleingrothaus, H. Päs, A.Yu. Smirnov, Phys. Rev. **D 63** (2001) 073005; H.V. Klapdor-Kleingrothaus, H. Päs, A.Yu. Smirnov, hep-ph/0103076 in Proc. DARK2000, July 10-15 2000, Heidelberg, Germany; S. Pascoli, S.T. Petcov, hep-ph/0205022; K. Matsuda, T. Kikuchi, T. Fukuyama, H. Nishiura, hep-ph/0204254; and references therein.
- [49] H.V. Klapdor-Kleingrothaus, A. Dietz, H.L. Harney, I.V. Krivosheina, Mod. Phys. Lett. **A16** (2001) 2409; compare however C.E. Aalseth *et al.*, hep-ex/0202018 and F. Feruglio, A. Strumia, F. Vissani, hep-ph/0201291; H.L. Harney, hep-ph/0205293; H.V. Klapdor-Kleingrothaus, hep-ph/0205228.
- [50] S. Sarkar, hep-ph/0202013; T.J. Weiler, hep-ph/0103023.
- [51] T.J. Weiler, Phys. Rev. Lett. **49** (1982) 234, and Astroparticle Phys. **11** (1999) 303; D. Fargion, B. Mele, A. Salis, Astrophys. J. **517** (1999) 725; T.J. Weiler, in “Beyond the Desert 99, Ringberg Castle”, Tegernsee, Germany, June 6-12, 1999.
- [52] Z. Fodor, S.D. Katz, A. Ringwald, Phys. Rev. Lett. **88** (2002) 171101, and JHEP 0206 (2002) 046; see also O. Kalashev *et al.*, hep-ph/0112351; G. Gelmini and G. Varieschi, hep-ph/0201273.